Citation for published version:
He, Y, Jiang, Y, Zhang, T, Ji, H, Wang, B, Huang, Z & Soleimani, M 2022, 'A new online monitoring method for water-in-oil droplet based microfluidic devices', *IEEE Sensors Journal*.
https://doi.org/10.1109/JSEN.2022.3181998

DOI:
10.1109/JSEN.2022.3181998

Publication date:
2022

Document Version
Peer reviewed version

Link to publication

© 2022 IEEE. Personal use of this material is permitted. Permission from IEEE must be obtained for all other users, including reprinting/ republishing this material for advertising or promotional purposes, creating new collective works for resale or redistribution to servers or lists, or reuse of any copyrighted components of this work in other works.

University of Bath

Alternative formats
If you require this document in an alternative format, please contact:
openaccess@bath.ac.uk

General rights
Copyright and moral rights for the publications made accessible in the public portal are retained by the authors and/or other copyright owners and it is a condition of accessing publications that users recognise and abide by the legal requirements associated with these rights.

Take down policy
If you believe that this document breaches copyright please contact us providing details, and we will remove access to the work immediately and investigate your claim.

Download date: 29. Jun. 2022

A new online monitoring method for water-in-oil droplet based microfluidic devices

Yuchen He, Yu He, Yandan Jiang, Tao Zhang, Haifeng Ji, Baoliang Wang, Zhiyao Huang, Manuchehr Soleimani

***Abstract*—The online water-in-oil (w/o) droplet monitoring is essential for the uniformity of the droplet based microfluidic devices. In this work, a ~~new~~ contactless impedance detection (CID) method for online w/o droplet monitoring in microfluidic devices is proposed. In the proposed method, a new CID sensor, which can work at low working frequency and overcome the unfavorable influence of coupling capacitance, is developed to obtain the impedance information of the w/o droplet. Based on the obtained impedance information, measurement models are established to realize online measurement of drop length and dispersed phase holdup. Then the coefficients of variation (CVs) of the two measured parameters are calculated to evaluate the uniformity of the droplets for online monitoring. Online monitoring experiments of w/o droplet were carried out in a microfluidic device with a 500 μm × 500 μm microchannel. The experimental results verify the effectiveness of the proposed droplet monitoring method. The ~~new~~ developed CID sensor can realize impedance measurement at a working frequency lower than 50kHz. The drop length and dispersed phase holdup are useful parameters for online monitoring of droplets. With the established measurement models, the maximum relative error of droplet length measurement is less than 10% in the droplet length range of 1.5mm-3.5mm. And the maximum error of dispersed phase holdup measurement is less than 5% in the dispersed phase holdup range of 0.20-0.67.**

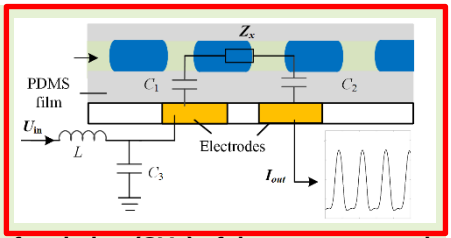

***Index Terms*—microfluidic, droplet monitoring, contactless impedance detection, droplet length, dispersed phase holdup**

I. Introduction

In the past two decades, droplet based microfluids has gradually become a significant category in the research field of microfluids. It can be used to fabricate intricate droplet based particles and generate droplets as microscale flow reactor [1-7]. Therefore, droplet based microfluidic devices which can generate water-in-oil (w/o) droplets have received great attention for applications in diagnostics, cellomics, proteomics, drug discovery and synthetic biology [3-6]. For these devices and applications, the parameter monitoring of droplets is important for the uniformity of the generation of droplets [5-8]. However, it is difficult and complicated to predict the parameters of droplets theoretically [1-9]. So, to better control the parameters of droplets, the online w/o droplet monitoring is essential for droplet based microfluidic devices [10-15].

Currently, optical methods such as laser-induced fluorescence, UV-vis absorption, infrared and Raman spectroscopies are commonly used methods for droplet monitoring [10-15]. These methods are non-invasive and have accurate measurement performance. But because they require off-chip instrumentation and are high-cost, they still cannot meet the growing requirements of online droplet monitoring in microfluidic devices [11-15]. In additional to optical methods, conductance detection methods are also used in microfluidic devices and they have good real-time performance [11-16]. However, conventional conductance detection methods are usually contact methods, which means the sensors are directly in contact with the fluid. That brings the drawbacks of polarization effect and electrochemical erosion [17-19]. Meanwhile, these contact sensors may disturb the generation and flow of the w/o droplets [10]. Besides, most of the contact conductance sensors are made of hydrophilic metal, which may cause unfavorable influence on the stability of the w/o droplets (the microchannel to generate and keep w/o droplets is supposed to be hydrophobic) [1-7]. So, to better meet the requirements of online w/o droplet monitoring in microfluidic devices, new monitoring methods, which can implement contactless measurement and has the advantages of good real-time performance, should be developed.

The emergence of contactless conductivity detection (CCD, also known as capacitively coupled contactless conductivity detection, C^4D) technique provides a new approach for online w/o droplet monitoring in microfluidic devices [17-20]. Because the electrodes of the CCD sensor ~~is~~ are not directly in contact with the fluid, the electrode polarization and electrochemical erosion effect can be avoided

This work was supported in part by the National Natural Science Foundation of China under Grant 61573312. (Corresponding author: Yandan Jiang).

Yuchen He, Yu He, Yandan Jiang, Tao Zhang, Baoliang Wang, Zhiyao Huang are with the State Key Laboratory of Industrial Control Technology, College of Control Science and Engineering, Zhejiang University, Hangzhou 310027, China (e-mail: hyc19940615@zju.edu.cn; hyhelen@zju.edu.cn; ydjiang@zju.edu.cn; zhtao@zju.edu.cn; wangbl@zju.edu.cn; zy_huang@zju.edu.cn).

Manuchehr Soleimani is with the Engineering Tomography Laboratory (ETL), Department of Electronic and Electrical Engineering, University of Bath, Bath BA2 7AY, UK (e-mail: M.Soleimani@bath.ac.uk).

XXXX-XXXX © XXXX IEEE. Personal use is permitted, but republication/redistribution requires IEEE permission.
See http://www.ieee.org/publications_standards/publications/rights/index.html for more information.

[17-29].

Up to now, the conventional CCD technique is mainly applied in the field of electrophoresis for ion concentration detection in capillaries [17-19]. The research works concerning the application of CCD technique in online w/o droplet monitoring – is limited [14-15, 20]. Cahill and co-workers extended the CCD technique to the contactless impedance detection (CID) technique and realized the online conductivity measurement of droplets in segment flow [20]. But in their work, the parameters of the droplet were not measured. Duarte and co-workers used an embedded CID sensor to measure the length of droplet [14]. But to reduce the capacitive reactance of the coupling capacitance, the working frequency of their sensor is was relatively high, which will increased the unfavorable influence of the stray capacitance on measurement results. Therefore, although the above pioneering research has achieved significant progress, the related research is not sufficient. To better apply CCD (CID) technique to online w/o droplet monitoring, more research work should be undertaken.

This work aims to proposes a CID method for online w/o droplet monitoring in microfluidic devices. By introducing an LC circuit, a new CID sensor is developed to obtain the impedance information of the w/o droplet. It can work at low working frequency and overcome the unfavorable influence of the coupling capacitance. With the obtained impedance information, droplet length measurement model and dispersed phase holdup measurement model will be developed for online measurement of droplet length and dispersed phase holdup of w/o droplets. Then, the coefficients of variation (CVs) of measured droplet length and dispersed phase holdup are calculated to evaluate the uniformity of the droplet and hence implement droplet monitoring. Online monitoring experiments of w/o droplets will be carried out to verify the effectiveness of the new proposed CID based monitoring method.

II. The Low-working Frequency CID Sensor In Microfluidic Devices

To show the universality of the proposed method, the microfluidic device used in this work was fabricated in a common way. A T-junction metal mold with a thickness of 500 μm was fabricated to facilitate the stripping of the polydimethylsiloxane from the mold. A portion (20 g) of PDMS prepolymers A and B with a ratio of 10:1 was poured on the mold. After baking at 85° for 90 minutes, a PDMS block with a T-junction channel was formed. All channels were with the width of 500 μm. After baking, the PDMS block with the channel was carefully peeled off from the mold and was punched three 1.5 mm holes, two as the inlets (one for continuous phase and the other for dispersed phase) and one as the outlet of the microfluidic chip. Then, the channel side of the PDMS block was bonded to a pre-prepared PDMS film with a thickness of 20 μm via oxygen plasma treatment to form the microfluidic chip shown in Fig.1a. Finally, the microfluidic chip and a pre-prepared PCB with two electrodes of the CID sensor (the widths of the two electrodes were 1 mm and the gap between the two electrodes was 0.5 mm) were both plasma-activated and bonded together to form the microfluidic device shown in Fig.1b. Between the channel and the electrodes, there is was a PDMS film with a thickness of 20 μm.

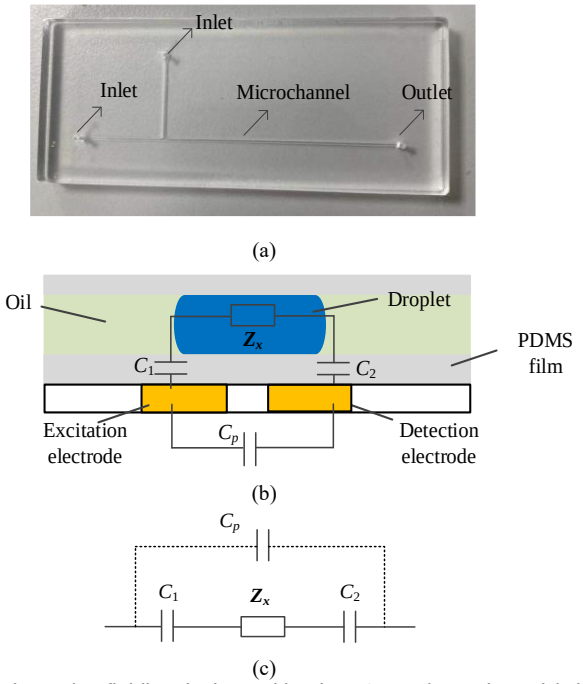

Fig.1. The microfluidic device with the CID electrodes. (a)The microfluidic chip: (b) The schematic diagram of integrated CID based microfluidic devices. (c) The equivalent circuit of the device.

By extending the conventional CCD technique to the CID technique, the fluid (droplets and oil) in the microchannel of microfluidic devices is considered as an impedance Z_x, as shown in Fig.1b-c. C_1 and C_2 are the coupling capacitances formed by the CID electrodes, the PDMS film and the conductive fluid in the microchannel. C_p is the stray capacitance formed directly by the two electrodes through air. From the viewpoint of impedance measurement, the impedance of the coupling capacitances $\frac{1}{j2\pi fC_1}+\frac{1}{j2\pi fC_2}$ and the stray capacitance $\frac{1}{j2\pi fC_p}$ are background impedance (f is the working frequency). They will cause unfavorable influence on the measurement results. Because coupling capacitances C_1 and C_2 are in series with Z_x, their unfavorable influence on the measurement results can be reduced by decreasing their impedance $\frac{1}{j2\pi fC_1}+\frac{1}{j2\pi fC_2}$. To decrease their impedance, a possible way is to increase the working frequency (this is the reason why the pioneering research works adopt high working frequency). In this way, both the impedance of coupling capacitances and the impedance of stray capacitance are decreased. However, because the stray capacitance C_p is in parallel with Z_x, its unfavorable influence on the measurement results will be greater with the decrease of its impedance $\frac{1}{j2\pi fC_p}$. That means the influence of stray capacitance which is small enough to be neglected at low working frequency is no longer negligible at high working frequency. So, increasing the working frequency is a contradictory approach. To ensure better measurement performance, it is necessary to seek a new approach that can 1) effectively overcome the unfavorable influence of the coupling capacitances, 2) enable the CID sensor to work at low working frequency to limit the unfavorable influence of the stray capacitance.

In this work, a new CID sensor which satisfies the above two

requirements is developed. Fig. 2 shows the construction of the ~~new~~ developed CID sensor.

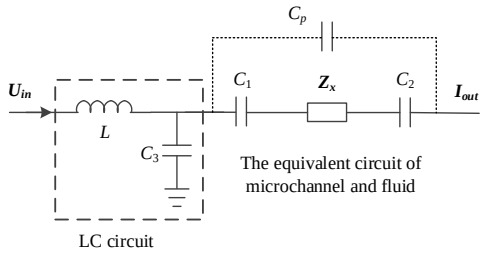

Fig.2. The construction of the new CID sensor.

In the ~~new~~ developed CID sensor, an LC circuit is introduced to the detection path to eliminate the influence of the coupling capacitances at a low working frequency. The LC circuit consists of an inductance L with an internal resistance R_L and a capacitance C_3. In the construction of the LC circuit, the AC source is connected to the introduced inductance module L. The introduced capacitance C_3 is grounded. The detection path is connected with the middle point of L and C_3.

According to Fig. 2, the output current $\boldsymbol{I_{out}}$ of the C^{4}D sensor is:

$$I_{out} = \frac{U_{in}}{\left(1+j2\pi fC_3\frac{(\frac{1}{j2\pi fC_1}+Z_x+\frac{1}{j2\pi fC_2})\frac{1}{j2\pi fC_p}}{\frac{1}{j2\pi fC_1}+Z_x+\frac{1}{j2\pi fC_2}+\frac{1}{j2\pi fC_p}}\right)\left(j2\pi fL+\frac{(\frac{1}{j2\pi fC_1}+Z_x+\frac{1}{j2\pi fC_2})\frac{1}{j2\pi fC_p}}{\frac{1}{j2\pi fC_1}+Z_x+\frac{1}{j2\pi fC_2}+\frac{1}{j2\pi fC_p}}\right)} \quad (1)$$

The impedance of stray capacitance $\frac{1}{j2\pi fC_p}$ is in parallel with the series of the impedance of coupling capacitance and the measured fluid $\frac{1}{j2\pi fC_1}+Z_x+\frac{1}{j2\pi fC_2}$. The impedance of a paralleled combination of the circuit is dominated by the by-pass with smaller impedance. In this work, because the values of coupling capacitance C_1 and C_2 are much greater than that of C_p and the working frequency is low, $\left|\frac{1}{j2\pi fC_p}\right| \gg \left|\frac{1}{j2\pi fC_1}+Z_x+\frac{1}{j2\pi fC_2}\right|$. Thus, the influence of the stray capacitance can be ignored. Therefore, in Eq. (1), $\frac{1}{j2\pi fC_1}+Z_x+\frac{1}{j2\pi fC_2}+\frac{1}{j2\pi fC_p} \approx \frac{1}{j2\pi fC_p}$ and $\frac{(\frac{1}{j2\pi fC_1}+Z_x+\frac{1}{j2\pi fC_2})\frac{1}{j2\pi fC_p}}{\frac{1}{j2\pi fC_1}+Z_x+\frac{1}{j2\pi fC_2}+\frac{1}{j2\pi fC_p}} \approx \frac{1}{j2\pi fC_1}+Z_x+\frac{1}{j2\pi fC_2}$. The output current $\boldsymbol{I_{out}}$ of the CID sensor in Eq. (1) can be simplified as:

$$\boldsymbol{I_{out}} = \frac{\boldsymbol{U_{in}}}{(1-4\pi^2f^2LC_3)\boldsymbol{Z_x} - j\frac{1}{2\pi fC_e}+j2\pi fL\frac{C_e+C_3}{C_e}} \quad (2)$$

Where $C_e = C_1C_2/(C_1+C_2)$ and $j\frac{1}{2\pi fC_e}$ is the background impedance introduced by coupling capacitances C_1 and C_2.

To eliminate the background impedance of coupling capacitance, $-j\frac{1}{2\pi fC_e}+j2\pi fL\frac{C_e+C_3}{C_e}$ should be zero. Let it be zero. This equation can be satisfied at the working frequency of:

$$f = \frac{1}{2\pi}\sqrt{\frac{1}{L(C_e+C_3)}} \quad (3)$$

At this working frequency, the overall impedance of the detection path is $(1-4\pi^2f^2LC_3)\boldsymbol{Z_x}$ and $\boldsymbol{I_{out}}$ is:

$$\boldsymbol{I_{out}} = \frac{\boldsymbol{U_{in}}}{(1-4\pi^2f^2LC_3)\boldsymbol{Z_x}} \quad (4)$$

Thus, according to Eq.(3) the amplitude of $\boldsymbol{I_{out}}$ is:

$$|\boldsymbol{I_{out}}| = \frac{|\boldsymbol{U_{in}}|}{(1-4\pi^2f^2LC_3)|\boldsymbol{Z_x}|} \quad (5)$$

Because L, C_3, f are constants (f is pre-determined by Eq.(3)), and $|\boldsymbol{U_{in}}|$ is also a constant. So, it can be known from Eq.(4) that the amplitude of $|\boldsymbol{I_{out}}|$ is inversely proportional to that of $|\boldsymbol{Z_x}|$. With the introduction of the LC circuit, the background impedance of coupling capacitance is eliminated. Meanwhile, according to Eq. (3), by adjusting the value of L and C_3, the CID sensor can work at low working frequency to limit the influence of stray capacitance to a negligible level.

III. The Response Of The New CID Sensor To Droplets

To verify the effectiveness of ~~new~~ the developed CID sensor, the response of the CID sensor to droplets is investigated. In this work, the value of L is set as 700.0mH, and the value of C_3 is set as 12.0 pF. The values of C_1 and C_2 are approximately 0.8 pF. According to Eq. (3), the working frequency is 48.65 kHz.

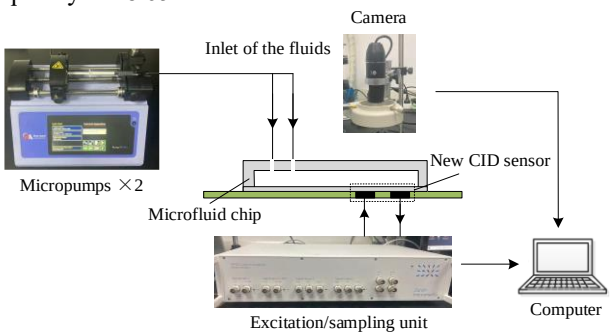

Fig.3. The experimental setup

Fig. 3 shows the experimental setup. Mineral oil with 3% EM90 was used as the continuous phase and aqueous solution with red food dye was used as the dispersed phase to generate the w/o droplets. Two syringe pumps (Pump 11 Elite, Harvard Apparatus) were used to pump the continuous phase and dispersed phase into the inlets of the microfluidic devices. After pumping these two fluids into the two inlets of the microfluidic devices, the w/o droplets were generated in the T-junction geometry, then flew downstream and passed through the electrodes of the CID sensor. A digital camera with microscope was used to capture the photos of the droplets and an excitation/sampling unit (Zurich Instruments) was connected with the CID sensor to provide excitation signal, record the impedance information, and send the data to the computer.

(a)

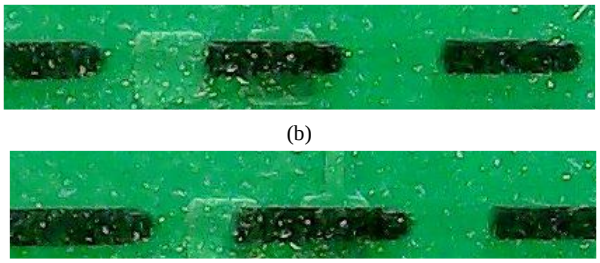

(b)

(c)

Fig.4. The droplets monitored at the continuous phase flow rate of 500 μL/h and three different dispersed phase flow rates: (a) Dispersed phase flow rate of 300 μL/h. (b) Dispersed phase flow rate of 500 μL/h. (c) Dispersed phase flow rate of 700 μL/h.

Fig. 4 shows the droplets monitored at the continuous phase flow rate of 500 μL/h and three different dispersed phase flow rates, captured by the digital camera. In Fig. 4, the oil phase is transparent, and the color of droplet looks black due to the red food dye. It can be known from Fig. 4 that the generation of droplets is relatively periodic. The length of droplets and the distance between the droplets are approximately constant. With the increase of the dispersed flow rate, the size of the droplets and the dispersed phase holdup in microchannel increase~~s~~. Meanwhile, as oil and water are incompressible fluids, the dispersed phase holdup in microchannel is approximately equal to the ratio of dispersed phase flow rate to the total flow rate (the sum of continuous phase flow rate and dispersed phase flow rate).

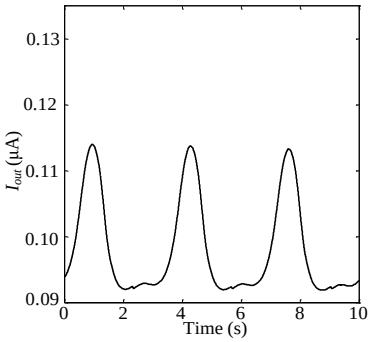

(a)

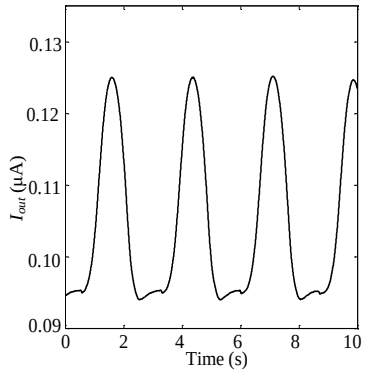

(b)

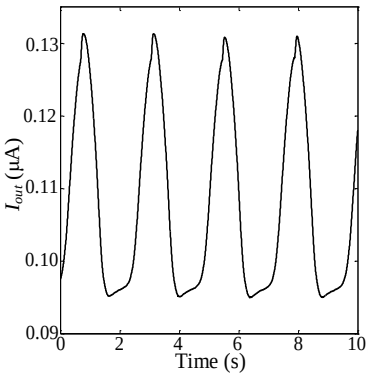

(c)

Fig.5. The impedance information (amplitude of the output current) obtained by the ~~new~~ developed CID sensor at the continuous phase flow rate of 500 μL/h and three different dispersed phase flow rates: (a) Dispersed phase flow rate of 300 μL/h. (b) Dispersed phase flow rate of 500 μL/h. (c) Dispersed phase flow rate of 700 μL/h.

Fig. 5 shows the impedance information obtained by the ~~new~~ developed CID sensor at the continuous phase flow rate of 500 μL/h and three different dispersed phase flow rates (corresponding to the conditions in Fig. 4). It can be known that the impedance information obtained by the CID sensor is also periodic and show good accordance with the observations from Fig. 4. Meanwhile, as shown in Fig. 5, a w/o droplet is detected as a positive peak in the output current signal obtained by the CID sensor. This is because the conductivity and permittivity of a droplet are higher than those of the mineral oil, which means the amplitude of the impedance of a droplet is smaller than that of the oil phase. So, the output current increases when a droplet-passes through the CID electrodes.

Besides, when the continuous flow rate is fixed at 500 μL/h, with the increase of the dispersed flow rate, the period of impedance information decreases. The height of each peak in the signal of the impedance information also increases (this result has also been obtained by Duarte and co-workers [14]).

above analysis shows that the development of the CID sensor is successful. The sensor can effectively realize the impedance measurement of w/o droplets in microfluidic device, at a low working frequency of 48.65 kHz. The impedance information measured by the CID sensor can reflect the parameters of the droplets, which indicates the potential of the sensor in online monitoring of droplets.

IV. New Online Monitoring Method For Water-in-oil Droplet Based Microfluidic Devices

The control of droplet length and monitoring of droplet uniformity are the key points of droplet-based microfluidic applications. To better control droplet length and monitor its uniformity, online monitoring is carried out with the-developed CID sensor. Because droplet length itself is the aim of control, and the drop length and dispersed phase holdup can reflect the uniformity of droplets, the online monitoring of w/o droplets here is on the basis of the online measurement of these two parameters.

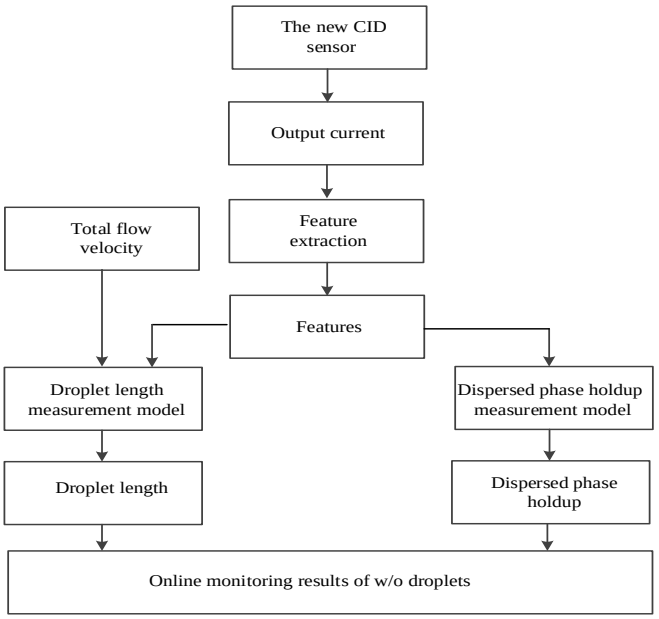

Fig.6. The scheme of the proposed online monitoring method.

Fig. 6 shows the scheme of the proposed online monitoring method. With the impedance information (amplitude of the output current) obtained by the ~~new~~ CID sensor, features which can reflect the interested parameters are extracted. With the features and the additional introduced total flow velocity, measurement model of droplet length is developed for online measurement of droplet length. Meanwhile, with the obtained features, measurement model of dispersed phase holdup is also developed for online measurement of dispersed phase holdup. With the online measurement results of droplet length and dispersed phase holdup, the uniformity of droplets is evaluated to implement the online monitoring.

A. The measurement of droplet length

To realize the measurement of droplet length with the output current of the CID sensor, the first step is to extract suitable features. Because the peaks of the output signal are resulted from the droplets, the parameters of peaks contain useful information of the droplet length and can be extracted as features. Among the characteristics of the peaks, peak width is a commonly used characteristic to reflect the volume of droplet [11, 14-15]. However, due to the complexity of contactless detection, the current output signal may slightly increase before the arrival of the droplet (at the position of the electrodes of the CID sensor). This brings difficulty ~~for~~ in finding the beginning and the end of a peak, and hence makes the peak width hard to determine. Therefore, instead of peak width, the full width at half maximum W is used as the feature to build the link between the output current signal and the droplet length. The full width at half maxima W is calculated ~~by~~ as the time difference ~~of~~ between the two points in one peak with the amplitude value~~s~~ of $(I_{max} + I_{min})/2$, as shown in Fig.7.

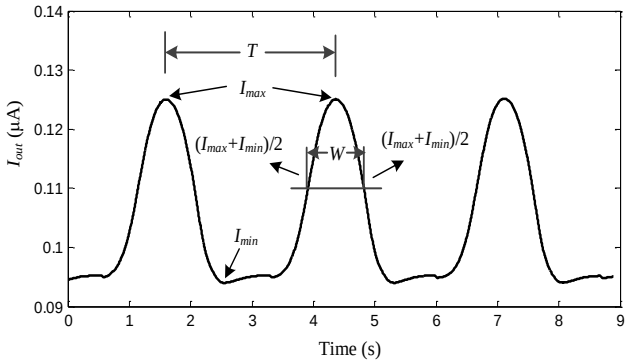

Fig.7. The features of the output current of the CID sensor.

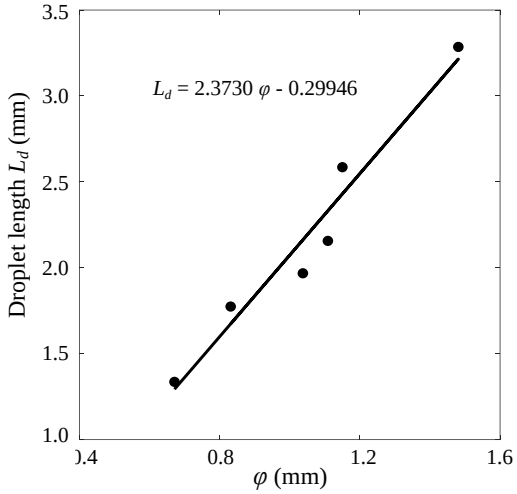

Fig. 8. The relationship between L_d and φ.

As the full width at half maximum W reflects the time that the droplet staying at the sensing position of the CID sensor, the product of full width at half maximum and the total flow velocity u_t, i.e., $\varphi = Wu_t$, can be used to establish the measurement model of drop length. To study the relationship between L_d and φ, preliminary experiments were carried out. The droplet length was changed by changing the flow rates of the continuous phase and the dispersed phase. The reference value of the droplet length is obtained from the photos of droplets captured by the digital camera. The total flow rate is obtained from the micropump. Fig. 8 shows the relationship between L_d and φ.

From Fig. 8, two-observations can be obtained: (1) The φ is relevant to the droplet length L_d. With the increase of L_d, -φ increases. (2) In the droplet length range of 1.2-3.3 mm, the relationship between φ and L_d shows good linearity. These indicate that the extracted feature is effective, and it is reliable to develop the droplet length measurement model with φ.

The pre-developed measurement model of droplet length is given in Fig. 8. Fig. 9 shows the flowchart to measure the droplet length in practical online monitoring. First, the full width at half maximum W is extracted from the output current of the CID sensor. With the extracted W and the introduction of the total flow velocity u_t, φ is obtained. Finally, with the obtained φ and the droplet length measurement model, the droplet length can be obtained.

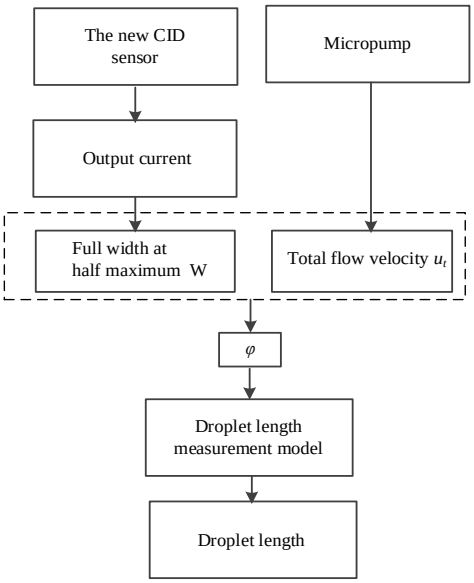

Fig.9. The flowchart to measure droplet length.

B. The measurement of dispersed phase holdup

The dispersed phase holdup α is the ratio of the dispersed phase volume to the total volume of the fluid. Because the oil and water are all incompressible fluids, this ratio is proportional to the ratio of dispersed phase flow rate to the total flow rate, i.e.

$$\alpha = \frac{Q_d}{Q_t} \tag{6}$$

Where Q_d is the flow rate of the dispersed phase. Q_t is the total flow rate calculated by:

$$Q_t = Q_d + Q_c \tag{7}$$

Where Q_c is the flow rate of the continuous phase.

Meanwhile, the generation of the droplets is generally periodic, and the oil and water are incompressible fluids, indicating that the dispersed phase holdup α is approximately equal to the ratio of the droplet volume V_d to the total volume of the fluid V_t in one period, i.e.

$$\alpha = \frac{V_d}{V_t} = \frac{V_d}{V_d + V_c} \tag{8}$$

Where V_c is the volume of the continuous phase in one period.

As the cross-sectional area of the channel is fixed, the volume of the droplet V_d in one period is approximately proportional to the length of droplet L_d in one period and the total volume in one period V_t is proportional to the total length of the fluid L_t in one period (the sum of the length of droplet and the length of the continuous phase between droplets), i.e.

$$V_d \approx SL_d \tag{9}$$

$$V_t \approx SL_t \tag{10}$$

Where S is the cross-sectional area of the channel.

By substituting Eq. (9) and Eq.(10) to Eq.(8), the dispersed phase holdup α can be rewritten as:

$$\alpha \approx \frac{SL_d}{SL_t} = \frac{L_d}{L_t} \tag{11}$$

As the droplet length can be calculated from φ, it is necessary to extract another feature that can reflect the total length L_t. Among the features of the output current signal, the time period T is one of the basic features. It reflects the frequency of droplet generation. So, the period T is extracted as another feature. L_t is approximately the product of the period T and the total velocity u_t:

$$L_t = Tu_t \tag{12}$$

Here, T is calculated by the time difference of the two nearest peak points with the value I_{max} in the amplitude of the output current, as shown in Fig.7.

Meanwhile, because L_t is equal to Tu_t in one period and the droplet length L_d is the linear function of Wu_t-the dispersed phase holdup can be calculated ~~just~~ from β, which is defined as the ratio of W to T:

$$\beta = \frac{Wu_t}{Tu_t} = \frac{W}{T} \tag{13}$$

That means the measurement of dispersed phase holdup can be realized without the introduction of the total flow velocity u_t.

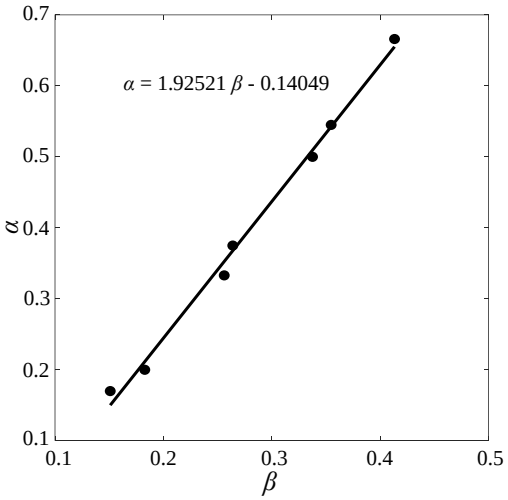

Fig. 10. The relationship between β and α

To study the relationship between β and α, preliminary experiments were carried out. Similarly, dispersed phase holdup is also changed by changing the flow rates of the continuous phase and the dispersed phase. The reference value of dispersed phase holdup is calculated as the ratio of the dispersed phase flow rate to the total flow rate (both obtained from the micropump). Fig.10 shows the relationship between β and α, with linear regression adopted. From Fig.10, again two observations can be obtained: (1) The ratio of the two extracted features β is relevant to the dispersed phase holdup α. With the increase of α, β increases. (2) In the dispersed phase holdup range of 0.17-0.67, the relationship between β and α shows good linearity. These indicate the effectiveness of the two extracted features and show that it is reliable to develop the model with β to realize dispersed phase holdup measurement.

The developed measurement model of the dispersed phase holdup is given in Fig.10. Fig.11 shows the flowchart to measure the dispersed phase holdup. With the impedance information of w/o droplet in the microchannel obtained by CID sensor, the time period T and full width at half maximum W are extracted and β is calculated. Then, with the dispersed phase holdup measurement model, the dispersed phase holdup can be obtained from β.

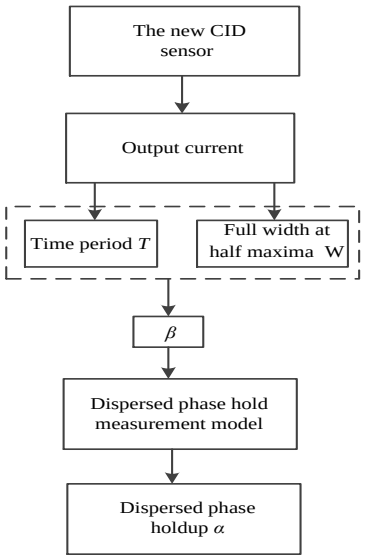

Fig.11. The flowchart to measure dispersed phase holdup.

C. The online monitoring of droplets

As aforementioned, the drop length and dispersed phase holdup can reflect the uniformity of droplets. Here, the online monitoring is implemented with the two parameters. The coefficients of variation (CVs) of the two parameters are used to evaluate the uniformity of the droplets. The definitions are:

$$CV_L = \frac{\sigma_L}{\mu_L} \tag{14}$$

$$CV_\alpha = \frac{\sigma_\alpha}{\mu_\alpha} \tag{15}$$

Where CV_L is the CV of the measured drop length and CV_α is the CV of the measured dispersed phase holdup. $\mu_L$and μ_α are the mean values of the measured droplet length and the dispersed phase holdup. σ_L and σ_α are the standard deviations of the measured droplet length and dispersed phase holdup, respectively. ~~And t~~The definitions of σ_L and σ_α are:

$$\sigma_L = \sqrt{\frac{1}{M-1}\sum_{m=1}^{M}(L_{dm}-\mu_L)^2} \tag{16}$$

$$\sigma_\alpha = \sqrt{\frac{1}{M-1}\sum_{m=1}^{M}(\alpha_m-\mu_\alpha)^2} \tag{17}$$

Where M is the number of measured droplets. L_{dm} and α_m are the measured droplet length and dispersed phase holdup of the mth droplets, respectively. m =1, 2, …, M.

With the two CVs, the droplets can be monitored. For most applications ~~for~~ of microfluidic devices, droplets with CV less than 3% can have good performance [7,15]. But in this work, the CVs calculated with the measured droplet length and dispersed phase holdup may not be equal to the actual CV of droplets. So, in practical monitoring, the quantitative standard of the two CVs to ensure a good uniformity may be different. To verify the effectiveness of the proposed ~~new~~ method and implement online monitoring of droplets, the correlation between the CVs of the two measured parameters and the uniformity of droplets (the actual CV of droplets) should be presented by experiment.

V. Experimental Results

A. Online measurement results of droplet length and dispersed phase holdup

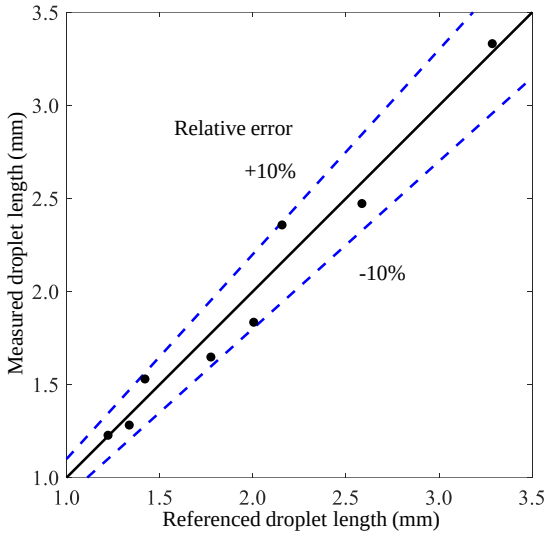

Fig.12.The online measurement results of droplet length.

To verify the effectiveness of the proposed method, practical online monitoring experiments were carried out. The range of dispersed phase flow rate~~s~~ was 200 to 700 μL/h and the range of the continuous phase flow rate ~~is~~ was 333 to 800 μL/h. Correspondingly, the investigated droplet length ~~is~~ was from 1.2 to 3.3 mm and the dispersed phase holdup ~~is~~ was from 0.2 to 0.67. Fig.12 shows the measurement results of droplet length. Fig.13 shows the measurement results of dispersed phase holdup.

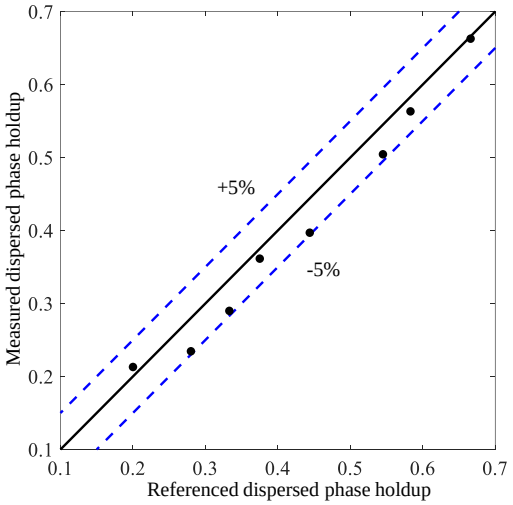

Fig.13. The online measurement results of dispersed phase holdup.

From Fig.12 and Fig.13, it is found that the measurement results of the two droplet parameters are in good agreement with the reference values. The time period and the full width at half maximum extracted from the output current of the CID sensor are useful features to realize droplet length measurement and dispersed phase holdup measurement. Experimental results show that the maximum relative error of droplet length

measurement is less than 10%-and the maximum measurement error of dispersed phase holdup measurement is less than 5%.

B. Online monitoring results of the w/o droplets

As mentioned above, the uniformity of the droplets is also the aim of monitoring and it is evaluated by the CVs of drop length and dispersed phase holdup. In the online monitoring experiment, the two CVs of the two measured parameters are calculated according to Eq.(14)-Eq.(17). Fig.14 and Fig.15 shows two examples of the generated w/o droplets in the experiment. The dispersed phase flow rate and continuous flow rate of Fig.14 are all 500 μL/h. The dispersed phase flow rate and continuous flow rate of Fig.15 are 500 μL/h and 700 μL/h, respectively.

Fig.14. A typical case in monitoring experiments (the dispersed phase flow rate and continuous flow rate are all 500 μL/h)

Fig.15. A typical case in monitoring experiments (the dispersed phase flow rate and continuous flow rate are ~~all~~ 700 μL/h and 500 μL/h, respectively).

For the case in Fig.14, the CVs of the measured droplet length and the dispersed phase holdup are 0.54% and 0.61%, respectively. It can be seen from Fig.14 that the uniformity is good (the actual CV of droplet length calculated from the photos of droplets is less than 3.0 %. Notation: 3.0 % is a widely used standard/threshold of the actual CV to evaluate the uniformity of the droplets [1-2, 7, 15, 32-33]. If the actual CV is less than 3.0 %, the droplets are regarded as uniform.). For the case in Fig.15, the CVs of the measured droplet length and the dispersed phase holdup are respectively 0.88% and 1.78 %, which are significantly higher than those of the case in Fig. 14. It can be seen from Fig.15 that the uniformity of this case is not as good as the case in Fig. 4 (the actual CV of droplet length calculated from the photo of droplets is greater than 3.0 %). So, for both the two cases, the value of the calculated CVs can reflect the actual uniformity of the droplets, which is in accordance with the actual CVs calculated from the photos. The CVs of the droplet length and dispersed phase holdup measured by the proposed method can reflect the actual uniformity of droplets, which means that the proposed method is effective.

Experimental results show that there exists approximate linear relationship between the calculated CV and the actual CV of the droplet length. Generally, for cases where the calculate CV is small, the actual CV is small. And, for cases where the calculate CV is large, the actual CV is large. However, the fluctuation and the discreteness of the experimental data are relatively large. At the current stage, it is difficult to develop the relationship rigorously. According to the current experimental conditions and the obtained experimental results, we have found that the value of 0.8% (of the calculated CV) could be regarded as a threshold/boundary value to ensure the uniformity of w/o droplets. If the value of the calculated CV is less than 0.8%, the corresponding actual CV is less than 3%, which ensures good uniformity of the droplets. It is indicated that the proposed method can qualitatively evaluate the uniformity of the droplets and implement online droplet monitoring.

VI. Conclusion

This work proposes a new CID based method for contactless online w/o droplet monitoring in microfluidic devices. In the ~~new~~ proposed method, a new CID sensor is developed to obtain the impedance information of the w/o droplet in microchannel. By introducing an LC circuit, the new CID sensor can overcome the unfavorable influence of coupling capacitance at low working frequency. With the obtained impedance information, two features (the full width at half maxima and the time period) are extracted to develop the measurement models of drop length and dispersed phase holdup. Online monitoring of w/o droplets is implemented by evaluating the variation of the measured drop length and dispersed phase holdup.

Online w/o droplet monitoring experiments were carried out in a T junction microfluidic device (500μm height and 500μm width). Experimental results verify the effectiveness of the proposed method. The CID sensor can obtain the impedance information of w/o droplets at low working frequency (48.65 kHz). The extracted features can effectively reflect the characteristics of the impedance information and the developed measurement models have good measurement performance. The maximum relative error for droplet length measurement is less than 10% in the drop length range from 1.2mm to 3.3mm. The maximum measurement error for dispersed phase holdup is less than 5% in the dispersed phase holdup range from 0.20 to 0.67. Results also indicate that the drop length and dispersed phase holdup are useful parameters for online monitoring of w/o droplets.

This work not only presents an online monitoring method for w/o droplet in microfluidic devices, but also provides an effective approach for dispersed phase holdup measurement in microfluidic devices. However, the research is not sufficient and more research should be undertaken in the future. To investigate the relationship between the calculated CVs and the actual CV, and to study the influence of experimental setup/conditions (such as parameters of the microchannel, geometrical parameters of the CID sensor, etc.) on this relationship will be our further research work.

References

[1] L. Shang, Y. Chen and Y. Zhao, Emerging Droplet Microfluidics, Chemical Review, vol. 117, no. 12, pp. 7964-8040, May 2017.
[2] J.S. Barea, J. Lee and D. Kang, Recent Advances in Droplet-based Microfluidic Technologies for Biochemistry and Molecular Biology, Micromachines, vol. 10, no. 6, pp. 412, Jun. 2019.
[3] S. Hardt and T. Hahn, Microfluidics with aqueous two-phase systems, Lab on a chip, vol.12, no. 3, pp.434-442, Mar. 2012.
[4] C. Yao, Y. Zhao and G. Chen, Multiphase processes with ionic liquids in microreactors: hydrodynamics, mass transfer and applications, Chemical Engineering Science, vol. 189, pp. 340-359, Nov. 2018.
[5] Y. Schaerli and F. Hollfelder, The potential of microfluidic water-in-oil droplets in experimental biology, Molecular BioSystems, vol.5, no.13, pp.1392-1404, Oct. 2009.
[6] E. Altamura, P. Carrara, F.D'Angelo, F. Mavelli,and P. Stano, Extrinsic stochastic factors (solute partition) in gene expression inside lipid vesicles and lipid-stabilized water-in-oil droplets: a review, Synthetic Biology, vol.3, no. 1, pp. ysy011, Jul. 2018,.

[7] K. Doufene, C. Tourne-Peteilh, P. Etienne, A. Aubert-Pouessel. Microfluidic systems for droplet generation in aqueous continuous phases: a focus review. Langmuir, vol. 35, no. 39, pp. 12597-12612, Oct. 2019.
[8] Z. Peng, G. Wang, B. Moghtaderi and E. Doroodchi. A review of microreactors based on slurry Taylor (segmented) flow. Chemical Engineering Science, vol. 247, pp. 117040, Jan. 2022.
[9] C. Yao, Y. Liu, C. Xu, S. Zhao and G. Chen. Formation of liquid-liquid slug flow in a microfluidic T-Junction: effects of fluid properties and leakage flow. AIChE Journal, vol.64, no.1, pp.346-357, Jan. 2018
[10] C.B. Kerr, R.W. Epps and M. Abolhasani. A low-cost, non-invasive phase velocity and length meter and controller for multiphase lab-in-a-tube devices. Lab on a Chip, vol.19, no. 12, pp.2107-2113, Apr. 2019.
[11] N. Antweiler, S. Gatberg, G. Jestel, J. Franzke and D.W. Agar. Noninvasive sensor for the detection of process parameters for multiphase slug flows in microchannels. Acs Sensors, vol.1, no. 9, pp. 1117-1123, Aug. 2016.
[12] J. Aubin, M. Ferrando and V. Jiricny. Current methods for characterising mixing and flow in microchannels. Chemical Engineering Science, vol. 65, no. 6, pp. 2065-2093, Mar. 2010.
[13] K. Burlage, C. Gerhardy, H. Praefke, M.A. Liauw and W.K. Schomburg. Slug length monitoring in liquid-liquid Taylor-flow integrated in a novel PVDF micro-channel. Chemical Engineering Journal, vol.227, pp.111-115, Jul. 2013.
[14] L.C. Duarte, C.L.S. Chagas, L.E.B. Ribeiro and W.K.T. Coltro, 3D printing of microfluidic devices with embedded sensing electrodes for generating and measuring the size of microdroplets based on contactless conductivity detection, Sensors and Actuators B: Chemical, vol.251, pp. 427-432, Nov. 2017.
[15] A. Saatch, A. Kalantarifard, O.T. Celik, M. Asghari, M. Serhatliglu and C. Elbueken, Real-time impedimetric droplet measurement (iDM), Lab on a Chip, vol.19, no.22, pp. 3815-3824, Nov. 2019.
[16] S. Liu, Y. Gu, R.B. Le Roux,S.M. Matthews, D. Bratton, K. Yunus, A.C. Fisher and W.T.S. Huck, The electrochemical detection of droplets in microfluidic devices, Lab on a Chip, vol. 8, no.11, pp.1937-1942, Sep. 2008.
[17] P. Kubáň and P.C. Hauser, 20th anniversary of axial capacitively coupled contactless conductivity detection in capillary electrophoresis, TrAC Trends in Analytical Chemistry, vol.12, pp. 311-321, May 2018.
[18] P. Kubáň and P.C. Hauser, Contactless conductivity detection for analytical techniques: Developments from 2016 to 2018, Electrophoresis, vol. 40, no.1, pp.124-139, Jan. 2019.
[19] 19.P. Kubáň and P.C. Hauser, Capacitively coupled contactless conductivity detection for analytical technique -Developments from 2018 to 2020, Journal of Chromatography A , vol.1632, pp. 461616, Nov. 2020.
[20] B.P. Cahill, R. Land, T. Nacke, M. Min and D. Beckmann, Contactless sensing of the conductivity of aqueous droplets in segmented flow, Sensors and Actuators B: Chemical, vol. 159, no.1, pp. 286-293, Nov. 2011.
[21] C. Huck, A. Poghossian, M. Bäcker, S. Chaudhuri, W. Zander, J. Schubert, V.K. Begoyan, V.V. Buniatyan, P. Wagner and M.J. Schöning, Capacitively coupled electrolyte-conductivity sensor based on high-k material of barium strontium titanate, Sensors and Actuators B: Chemical, vol. 198, pp. 102-109, Jul. 2014.
[22] Z. Huang, W. Jiang, X. Zhou, B. Wang, H. Ji and H. Li, A new method of capacitively coupled contactless conductivity detection based on series resonance, Sensors and Actuators B: Chemical, vol.193, no.1, pp.239-245, Dec. 2009.
[23] P. Tůma, Determination of amino acids by capillary and microchip electrophoresis with contactless conductivity detection-Theory, instrumentation and applications, Talanta, vol.224, pp.121922, Mar.2021.
[24] K.J.M. Francisco and C.L.A. do Lago, Compact and high-resolution version of a capacitively coupled contactless conductivity detector, Electrophoresis, vol.30, no. 19, pp.3458-3464. Oct. 2009.
[25] W.K.T. Coltro, R.d.S. Neves, A.d.J. Motheo, J.A.F. da Silva and E. Carrilho, Microfluidic devices with integrated dual-capacitively coupled contactless conductivity detection to monitor binding events in real time, Sensors and Actuators B: Chemical, vol.192, pp. 239-246.Mar. 2014.
[26] R.F. Quero, L.P. Bressan, J.A.F. da Silva and D.P. de Jesus, A novel thread-based microfluidic device for capillary electrophoresis with capacitively coupled contactless conductivity detection, Sensors and Actuators B: Chemical , vol. 286, pp.301-305, May 2019.
[27] F. Opekar and P. Tůma, A simple impedance tester for determining the water content in organic solvents, Sensors and Actuators B: Chemical, vol.220, pp. 485-490, Dec. 2015.
[28] M. Pumera, Contactless conductivity detection for microfluidics: designs and applications, Talanta, vol.74, no.3, pp.358-364, Dec. 2007.
[29] R.S. Lima, T.P. Segato, A.L. Gobbi, W.K. Coltro and E. Carrilho, Doping of a dielectric layer as a new alternative for increasing sensitivity of the contactless conductivity detection in microchips, Lab on a Chip, vol.11, no. 24, pp. 4148-4151, Nov. 2011.
[30] M. Zhang, B.N. Stamos, N. Amornthammarong, P.K. Dasgupta, Capillary scale admittance detection, Analytical Chemistry, vol.86, no.23, pp.11538-11536, Oct. 2014.
[31] M. Zhang, B.N. Stamos, P.K. Dasgupta, Admittance detector for high impedance systems: Design and applications, Analytical Chemistry, vol.86, no.23, pp.11547-11553, Oct. 2014.
[32] Z. Lian, Y. Chan, Y. Luo, X. Yang, K.S. Koh, J. Wang, G.Z. Chen, Y. Ren, and J. He. Microfluidic formation of highly monodispersed multiple cored droplets using needle-based system in parallel mode. Electrophoresis, vol.41, no.10-11, pp. 891-901, Jun, 2020.
[33] E. Amstad, M. Chemama, M. Eggersdorfer, L.R. Arriaga, M.P. Brenner and D.A. Weitz. Robust scalable high throughput production of monodisperse drops. Lab on a chip, vol. 16, no. 21, pp. 4163-4172, Nov. 2016.

Yuchen He was born in Hangzhou, China, on June 15, 1994. He received the B.Sc. degree from Northwest A&F University, Xi'an, China, 2016. He is currently working toward the Ph.D degree with the College of Control Science and Engineering, Zhejiang University. His research interests include measurement technology, automatic equipment and microfluidic devices.

Yu He obtained her B.Sc. degree from Xiamen University, Fu jian, China, 2016. She is currently working toward the Ph.D degree with the College of Control Science and Engineering, Zhejiang University, China. Her research interests involve droplet microfluidics, digital microfluidics and development of microfluidic devices for biochemical analysis.

Yandan Jiang was born in Jinhua, China, on February 14, 1992. She received the B.Sc. degree from Zhejiang University of Technology, Hangzhou, China, in 2013 and the Ph.D. degree from Zhejiang University, Hangzhou, China, in 2019. From Oct. 2017 to Oct. 2018, she worked as a visiting Ph.D. with the Department of Electronic and Electrical Engineering, University of Bath, Bath, UK. She is currently an Associate Researcher with the College of Control Science and Engineering, Zhejiang University, China. Her research interests include automation instrumentation, multiphase flow measurement techniques, process tomography and biomedical imaging.

Tao Zhang obtained his B.Sc in Chemical Engineering and Technology from Jilin University (2002). He received his Ph.D in Measuring Technology and Instrumentation from Jilin University (2007). He is currently associate professor of Measuring Technology and Automation Equipment at Zhejiang University, China. His research interests involve photofabrication of microfluidic device, droplet microfluidics and digital microfluidics for bioananlysis.

Haifeng Ji was born on 26 October 1973 in China. He received his master degree from Shandong University of Technology in 1999 and his Ph.D. degree from Department of Control Science and Engineering, Zhejiang University, in 2002, respectively. Now he is working in Zhejiang University as an Associate Professor. His interesting research includes measurement techniques, automation equipment, information processing of complex process system, multiphase flow measurement in mini-/micro-channel.

Baoliang Wang was born in Zibo, China, on July 11, 1970. He received the B.Sc. and M.Sc. degrees from Shandong University of Technology, Jinan, China, in 1992 and 1995, respectively. In 1998, he received the Ph.D. degree from Zhejiang University, Hangzhou, China. From 1998 to 2001, he was a Lecturer with the Department of Control Science and Engineering, Zhejiang University. From 2002 to 2003, he was a research associate at the City University of Hong Kong. From 2002 to 2013, he was an Associate Professor with the Department of Control Science and Engineering, Zhejiang University. Since 2014, he was appointed as a Professor with the department of Control Science and Engineering, Zhejiang University. His research interests include process tomography, motion control system, microprocessor application.

Zhiyao Huang was born in Hangzhou, China, on October 22, 1968. He received the B.Sc., M.Sc., and Ph.D. degrees from Zhejiang University, Hangzhou, China, in 1990, 1993, and 1995, respectively. From June 1995 to August 1997, he was a Lecturer with the Department of Chemical Engineering, Zhejiang University. In September 1997, he became an Associate Professor with the Department of Control Science and Engineering, Zhejiang University, and in 2001, he was appointed a Professor. Currently, he is a Professor with the College of Control Science and Engineering, Zhejiang University. He is also a permanent staff of the State Key Laboratory of Industrial Control Techniques. His current interests include automation instrumentation and multiphase flow measurement.

Manuchehr Soleimani received the B.Sc. degree in electrical engineering and the M.Sc. degree in biomedical engineering, and the Ph.D. degree in inverse problems and electromagnetic tomography from The University of Manchester, Manchester, U.K., in 2005. From 2005 to 2007, he was a Research Associate with the School of Materials, The University of Manchester. In 2007, he joined the Department of Electronic and Electrical Engineering, University of Bath, Bath, U.K., where he was a Research Associate and became a Lecturer, in 2008, a Senior Lecturer, in 2013, a Reader, in 2015, and a Full Professor, in 2016. In 2011, he founded the Engineering Tomography Laboratory (ETL), University of Bath, working on various areas of tomographic imaging, in particular multimodality tomographic imaging. He has authored or co-authored well over 300 publications in the field.